第 31 卷第 8 期 无 机 化 学 学 报 Vol.31 No.8
2015 年 8 月 CHINESE JOURNAL OF INORGANIC CHEMISTRY 1626-1636

# 多级结构氧化锌的构筑、形貌调控及其光催化活性

全微雷 张金敏 沈俊海 李良超* 李佳佳
(浙江师范大学化学与生命科学学院,金华 321004)

**摘要**:分别以混合常见二锌盐为锌源,以离子液体和柠檬酸钠为表面活性剂,在绿色温和的条件下采用二次沉积法制备出多级结构氧化锌。用 XRD、IR、SEM、UV-Vis、PL 等表征了样品的组成、结构、形貌、光致发光性能及光催化性能。探讨了表面活性剂、阴离子、温度等因素对氧化锌形貌的影响。结果表明,由不同表面活性剂所得到样品的多级结构有较大的差异。此外,推测了在多级结构氧化锌形成过程中,阴离子和温度对样品形貌的调控作用,并对比了三种典型样品的光催化性能,其中样品-1 的光催化性能最好。

**关键词**:氧化锌;多级结构;形貌调控;光催化
**中图分类号**:O614.24+1 **文献标识码**:A **文章编号**:1001-4861(2015)08-1626-11
**DOI**:10.11862/CJIC.2015.212

## Hierarchical ZnO: Architecture, Morphological Control and Photocatalytic Activity

QUAN Wei-Lei ZHANG Jin-Min SHEN Jun-Hai LI Liang-Chao* LI Jia-Jia
(*College of Chemistry and Life Sciences, Zhejiang Normal University, Jinhua, Zhejiang* 321004, *China*)

**Abstract:** Under the green and mild conditions, the hierarchical ZnO was fabricated by the secondary deposition with mixed two zinc salts (zinc source), ionic liquid (surfactant). The composition, structure, morphology, photoluminescence properties and photocatalytic activity of samples were characterized by XRD, IR, SEM, UV-Vis and PL, respectively. The influential factors on sample morphology, such as surfactant, the kind of anion and temperature, were discussed. The results indicate that surfactant has a significant regulation on the morphologies of as-prepared ZnO samples. Furthermore, the anion and temperature also play a critical role in the crystal structure and morphology of ZnO. In addition, all of as-prepared hierarchical ZnO show an excellent photocatalytic activity on methyl orange under UV lamp, where the sample-1 is slightly better than others.

**Key words:** ZnO; hierarchical structure; morphological control; photocatalysis

## 0 Introduction

Due to the special microstructure and physico-chemical properties, inorganic micro-nano materials with different microscopic sizes and morphologies have been widely applied in optics, electricity, magnetism, biological medicine, catalysis, and other fields[1-4]. Furthermore, with the improvement of application demands, the control on material microscopic morphology has been paid much attention[5-6]. As one of the most important semiconductor materials, ZnO has emerged as one of the most promising candidate materials owing to its superior properties and the potential advantage in future electron device[7-10]. According to the principle that material properties depend on its structure, researchers have devoted themselves

收稿日期:2015-04-21。收修改稿日期:2015-06-29。
国家自然科学基金(No.21071125)和浙江省大学生科技创新计划(No.2014R404056)资助项目。
*通讯联系人。E-mail:sky52@zjnu.cn;会员登记号:S06N6780M1401。

to the controllable synthesis of materials with different microscopic morphologies and sizes. For example, Ma et al[11] reported three kinds of ZnO with different morphologies and found that they possessed various photocatalytic activities on methyl orange, in which the nanorod-like ZnO has the best photocatalytic activity, the flower-like ZnO is the second, and the nanoparticle ZnO is the worst. In addition, much more different morphologies of ZnO have been reported, such as mesoporous spheres, tubular, four foot shape and fibrous, etc[12-16], in which most researches are about ZnO nanoparticles and nanoplates. However, to the best of our knowledge, there have been no reports on the hierarchical ZnO constructed by two morphologies.

A lot of micro-nano structure in the nature usually shows some inconceivable function. For example, the micro-nano structure on the surface of lotus leaf makes it have super hydrophobic and self-cleaning function. The micro-nano structure on the leg of water flies makes it walk on the water freely[17]. So the micro-nano structure has infinite mystery. However, whether the hierarchical ZnO assembled by micro-nano structure has the unusual photocatalytic activity? It is a pity that the reports associated with the above question are very little, the main reason is that it is very difficult to fabricate the well-defined micro-nano structure and to control its morphology effectively. The Chemical Vapor Deposition (CVD) method has been paid attention owing to its high efficiency [18-19]. However, the CVD method needs high temperature and can introduce impurities. There are very few reports [20-22] about the simple fabrication of hierarchical ZnO, especially under the green and mild preparation conditions.

Besides, in regard to the regulation of ZnO microstructure, the single zinc salt is often used as the zinc source to fabricate ZnO[23-24], and some common surfactants (e.g. CTAB, PVP, etc.) are used as the template agent or structure-directing agent[25-26]. However, these surfactants are difficult to be removed completely in the post-processing, which may have negative effect on ZnO performance, due to the reduction in the polarization plane of ZnO. But the ionic liquid (IL) as a kind of green solvent has been applied in the fabrication of inorganic micro-nano materials including ZnO[27-28], which can work as the co-surfactant and be removed easily.

Thus we choose the mixed zinc salts as the zinc source. Beacuse the anions in zinc salts have various spatial structures and electronegativities, ZnO seed may have different absorption capacities to them, so they can affect the crystal growth to adjust ZnO morphology. On the other hand, the introduction of IL can improve the solubility of inorganics and organics, and IL can play a role as the special surfactant. More importantly, the effect of IL on ZnO morphology can be studied by changing the anion in IL. Herein, we report the ZnO with hierarchical structure by a simple and green secondary deposition method. Based on our previous work[29], it is expected to fabricate the hierarchical ZnO with well-organized micro-nano structures, i.e., micro-sized ZnO grains are coated by ZnO nanoparticles. In this paper, the precursor solution including the micro-sized ZnO grains is obtained by hydrothermal method. Then the pH value of the precursor solution is adjusted by NaOH solution under the room temperature, the residual $Zn^{2+}$ ions can form ZnO on the surface of micro-sized ZnO grains. As a result, the prepared hierarchical ZnO consists of the micro-sized ZnO grains fabricated by hydrothermal method and the coating layer of nano-sized ZnO particles obtained by the secondary deposition. Furthermore, some influential factors on the morphology of hierarchical ZnO, such as the kind of anion in zinc salt, surfactants and reaction temperature are studied. In addition, the photocatalytic activity of three kinds of morphological ZnO on methyl orange (MO) is also studied.

## 1 Experimental

### 1.1 Materials

Zinc acetate ($Zn(CH_3COO)_2\cdot 2H_2O$), Zinc sulfate ($ZnSO_4\cdot 7H_2O$), Zinc chloride ($ZnCl_2$), Zinc nitrate ($Zn(NO_3)_2\cdot 6H_2O$), NaOH, $C_3H_7NO_2$, $C_2H_5OH$, Sodium citrate ($C_6H_5Na_3O_7\cdot 2H_2O$) were all of analytical purity

provided by the Shanghai Sinopharm Chemical Reagent Co., Ltd. and were used as received without further purification. [BMIM]Cl, [BMIM]Br and deionized water were prepared by this laboratory.

### 1.2 Sample preparation

1.2.1 Fabrication of precursor solution

[BMIM]Cl and [BMIM]Br were synthesized following the literature procedures[30-31].

The preparation procedure is as follows: 1 mmol $Zn(CH_3COO)_2 \cdot 2H_2O$ and 1 mmol $ZnCl_2$ were dispersed in a mixed solution consisting of 30.0 mL deionized water and 2 mmol [BMIM]Br to form white turbid solution. Then 2 mmol alanine was added into the above solution, stirred until a clear solution was obtained. 4 mmol NaOH was added into the clear solution under vigorous stirring. A white colloidal turbid liquid was finally obtained and transferred into a Teflon-lined stainless autoclave (volume of 50.0 mL). Then the autoclave was heated and maintained at 150 ℃ for 15 h, the precursor solution was obtained after cooling down the system to room temperature.

1.2.2 Fabrication of the sample-1

1 mol·$L^{-1}$ NaOH solution was added dropwise into 25 mL of the above precursor solution until the precipitation was formed completely. After filtering, the solid precipitation was washed three times with deionized water and ethanol. Then, the sample-1 was obtained by drying to constant weight under vacuum at 50 ℃. By changing the zinc salt, surfactants and reaction temperature, other ZnO samples in different morphologies were obtained by the same method.

### 1.3 Photocatalytic studies

Methyl orange (MO) was used as the simulative pollutant to evaluate the photocatalytic activity of the as-prepared samples by standard curve method. In a typical experiment, 3 mmol sample-1 was dispersed uniformly in 100 mL MO solution with 12 mg·$L^{-1}$ by ultrasonication. The above mixture was irradiated under UV lamp (3×8 W). 3 mL suspension was taken out from the reaction system every 10 min, and immediately centrifuged. The absorbance of centrifugal solution was measured by a UV-Vis spectrophotometer at $\lambda_{max}$=465 nm.

In addition, the influence of ZnO dosage on photocatalytic activity was studied. A certain amount of sample-1 was uniformly dispersed in 100 mL MO solution with 12 mg·$L^{-1}$ by ultrasonication, which was irradiated under UV lamp (3×8 W). After 80 min, the dagradation rate of MO was measured by a UV-Vis spectrophotometer at $\lambda_{max}$=465 nm.

### 1.4 Characterization

The phase structure of the sample was characterized using an X-ray diffractometer (Philips-PW3040/60) with Cu $K\alpha$ radiation ($\lambda$=0.154 18 nm, 10°·$min^{-1}$, $U$=40 kV, $I$=40 mA, Ni filter) in the range of $2\theta$=10°~80°. The infrared spectrum was recorded on the Nicolet Nexus 670 Fourier transform infrared spectrometer (FTIR) using KBr pellets (scan range of 400~4 000 $cm^{-1}$). The morphologies and microstructures were observed by a scanning electron microscopy (SEM, Hitachi S-4800, $U$=5.0 kV). The UV-Vis absorption of MO solution was measured with an ultraviolet-visible spectrophotometer (Shmadzu UV-2501PC). A photoluminescence (PL) spectrum of the sample-1 was recorded in an FL-920 fluorescence spectrophotometer in wavelength of 325 nm. The organic carbon of MO solution was measured by Total Organic Carbon Analyzer (ELEMENTAR Liqui TOC Ⅱ).

## 2 Results and discussion

### 2.1 X-ray diffraction

The XRD pattern of sample-1 is presented in Fig.1. The strong and sharp diffraction peaks demonstrate that sample-1 has good crystallization. In addition, all peaks are in agreement with the characteristic

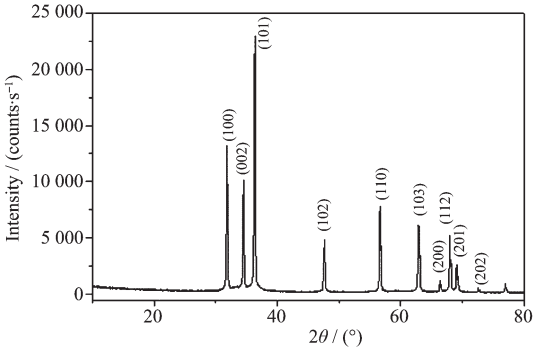


Fig.1 XRD pattern of the sample-1

peaks of hexagonal ZnO (PDF-2 No 36-1451), and correspond to (100), (002), (101), (102), (110) and (103) crystal face. No diffraction peaks of impurities are observed, which illustrates that the as-prepared sample-1 is highly pure.

## 2.2 FTIR spectra

Fig.2 shows the FTIR spectra of sample-1. The bands at 435 and 534 $cm^{-1}$ are attributed to Zn-O axial stretching vibration[32]. The band at 3 432 $cm^{-1}$ is assigned to -OH stretching vibration, which may be caused by the absorbed $H_2O$ on the surface of sample-1. The band at 1 099 $cm^{-1}$ is assigned to C-O stretching vibration. In addition, the weak bands at 1637 and 1 384 $cm^{-1}$ correspond to anti-symmetric and symmetric stretching vibration of $COO^-$, suggesting that the $CH_3COO^-$ groups are absorbed on the ZnO grain surface and there may be some coordination bonds between the $Zn^{2+}$ and $CH_3COO^-$.

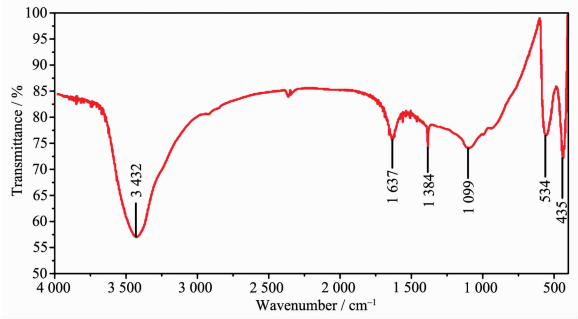


Fig.2　FTIR spectrum of the sample-1

## 2.3 Morphology

The SEM images of sample-1 are shown in Fig.3. The ZnO particles possess a hierarchical structure with etching decorative pattern, indicating a high surface area. The high-resolution image (Fig.3b) clearly shows that the well-bedded surface of hierarchical ZnO is constructed by nanoparticles of 50~100 nm, and has agglomeration to some extent. Some of these nanoparticles keep spherical morphology, while other shows the irregular morphology due to serious reunion.

### 2.3.1 Influence of surfactant on the sample morphology

Surfactant can regulate and control the nucleation and assembling of ZnO nanoparticles[33]. In addition, due to the changes in spatial structure, solubility and functional groups of surfactants, the special regulating and controlling effect is different. Therefore, to investigate the effect of surfactants (IL and sodium citrate), the kind and dosage of the surfactant are considered. The experimental parameters and sample morphologies are given in Table 1 (in section 1.2.2) and Fig.4, saparately.

The morphological differences are evident. For example, sample-2 presents the irregular spherical aggregates formed by nanospheres with 100~150 nm, and the nanospheres are actually assembled by the smaller spherical nanoparticles with 10~20 nm. While the irregular nanospheres convert to the triangulated petals, when the [BMIM]Cl is replaced by 1 mmol sodium citrate. So the flower-like ZnO (sample-3) is well revealed in Fig.4b, which is constituted by a pistil and some petals with rugged surface due to the adhesion ZnO nanoparticles. Here one can reasonably speculate that the pistils and petals are assembled by ZnO nanoparticles according to the specific orientation. Moreover, combining [BMIM]Cl with sodium citrate for sample-4, the prepared ZnO

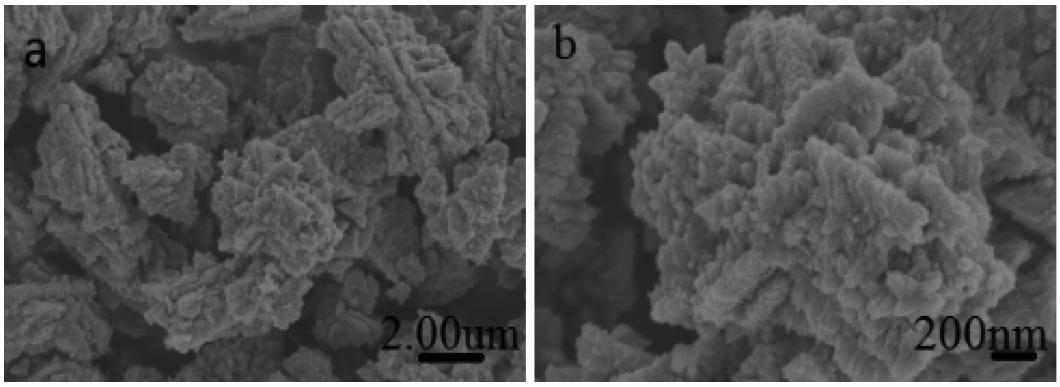


Fig.3　SEM images of the sample-1

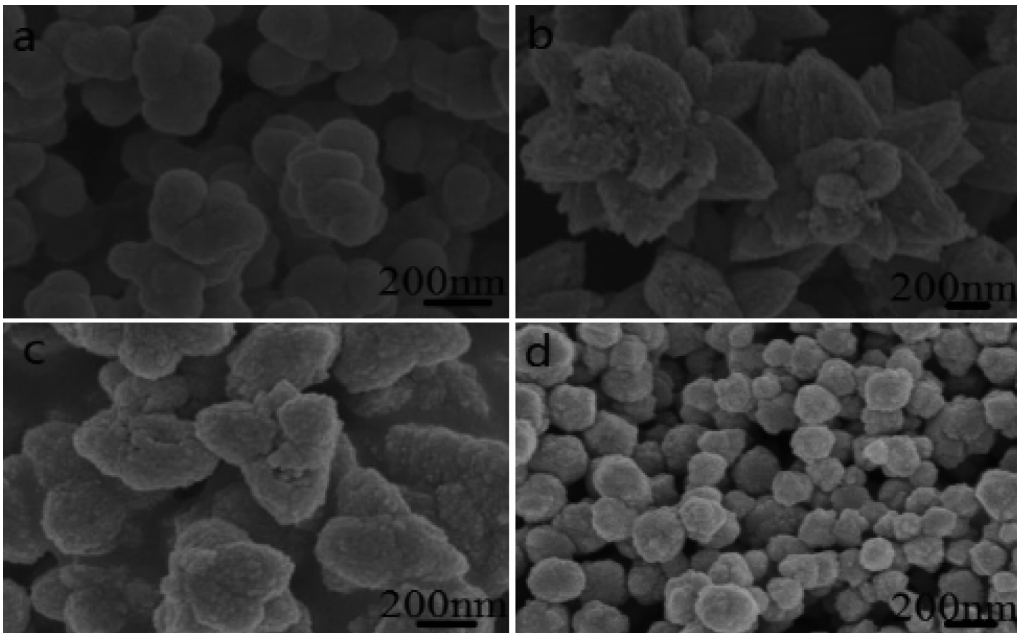


Fig.4 Effect of surfactants on ZnO sample morphology

presents multi-foot structure (Fig.4c). In fact, the ZnO nanoparticles adhere on the surface of every foot, and the cone-like foot end is similar to the strawberry. At last, the ZnO nanospheres (sample-5) with the size of 100~200 nm (Fig.4d) are obtained without any IL and sodium citrate, their surface is unsmooth due to being covered by the smaller particles. Compared Fig.4a and 4d, their size and morphology are similar, but the dispersity of the latter (Fig.4d) is better.

The above results indicate that the surfactant plays a critical role in the formation process of hierarchical ZnO. No matter what the molar ratio of ILs to sodium citrate is, the minimum basic unit of all obtained samples is nanoparticles. However, the fundamental difference among above as-obtained samples attributes to the interaction forces among nanoparticles, leading to different orientations of nanoparticles in the process of self-assembly, which illustrates that IL and sodium citrate have some influence on self-assembly kinetics of nanoparticles, or have the specific effect as template, structure oriented agent or both on the assembling of nanoparticles. The hierarchical structure of sample-1 has the biggest size and the most complicated morphology. By contrast, sample-5 prepared without any surfactant is the smallest in the size, and it presents simple spherical structure, which is the most common morphology caused by nanoparticles reunion. In addition, comparing sample-3 and sample-4, the arrange orientation of nanoparticles disappears completely, because of the replacement of [BMIM]Br by [BMIM]Cl. Thus, it can be concluded that the auxiliary effect of [BMIM]Cl on nanoparticle assembly is poorer than that of [BMIM]Br. It may because that the $Cl^-$ has a larger electronegativity and a smaller ionic radius compared with that of $Br^-$, i.e., $Cl^-$ has a weaker ability of donating electrons. However, the introduction of sodium citrate is helpful for nanoparticles to arrange orderly (Fig.4b), and the effect of sodium citrate as the template agent (or structure oriented agent) is much better compared with that of [BMIM]Br. It is because that $CH_3COO^-$ is more easily to combine with $Zn^{2+}$ as confirmed by FTIR. Moreover, when [BMIM]Cl is substituted for [BMIM]Br, the template effect of sodium citrate becomes weakened drastically, which also proves that [BMIM]Cl cannot work as the template. In addition, $Cl^-$ with a big electronegativity also weakens the template effect of sodium citrate. To sum up, the template effect of sodium citrate is the best, while that of the [BMIM]Cl is the worst among three surfactants in terms of constructing hierarchical ZnO.

2.3.2 Influence of zinc source on the sample morphology

Only the zinc source is changed in the following experiments. The precursor solutions with different mixed zinc salts are designed as shown in Table 1.

The ZnO morphologies and structures prepared by different zinc sources are shown in Fig.5. The ZnO morphologies and structures are closely related to the

**Table 1　Experimental parameters for different sample**

| Sample code | Zinc salt (1 mmol each) | IL / mmol | Sodium citrate / mmol | Temperature / ℃ | Morphology |
|---|---|---|---|---|---|
| 1 | Zinc acetate+zinc chloride | 2 [BMIM]Br | 0 | 150 | Fig.3 |
| 2 | Zinc acetate+zinc chloride | 1 [BMIM]Br+1 [BMIM]Cl | 0 | 150 | Fig.4a |
| 3 | Zinc acetate+zinc chloride | 1 [BMIM]Br | 1 | 150 | Fig.4b |
| 4 | Zinc acetate+zinc chloride | 1 [BMIM]Cl | 1 | 150 | Fig.4c |
| 5 | Zinc acetate+zinc chloride | 0 | 0 | 150 | Fig.4d |
| 6 | Zinc acetate+zinc sulfate | 2 [BMIM]Br | 0 | 150 | Fig.5(a+b) |
| 7 | Zinc acetate+zinc nitrate | 2 [BMIM]Br | 0 | 150 | Fig.5(c+d) |
| 8 | Zinc chloride+zinc nitrate | 2 [BMIM]Br | 0 | 150 | Fig.5(e+f) |
| 9 | Zinc chloride+zinc sulfate | 2 [BMIM]Br | 0 | 150 | Fig.5(g+h) |
| 10 | Zinc acetate+zinc chloride | 2 [BMIM]Br | 0 | 120 | Fig.6(a+b) |
| 11 | Zinc acetate+zinc chloride | 2 [BMIM]Br | 0 | 180 | Fig.6(c+d) |

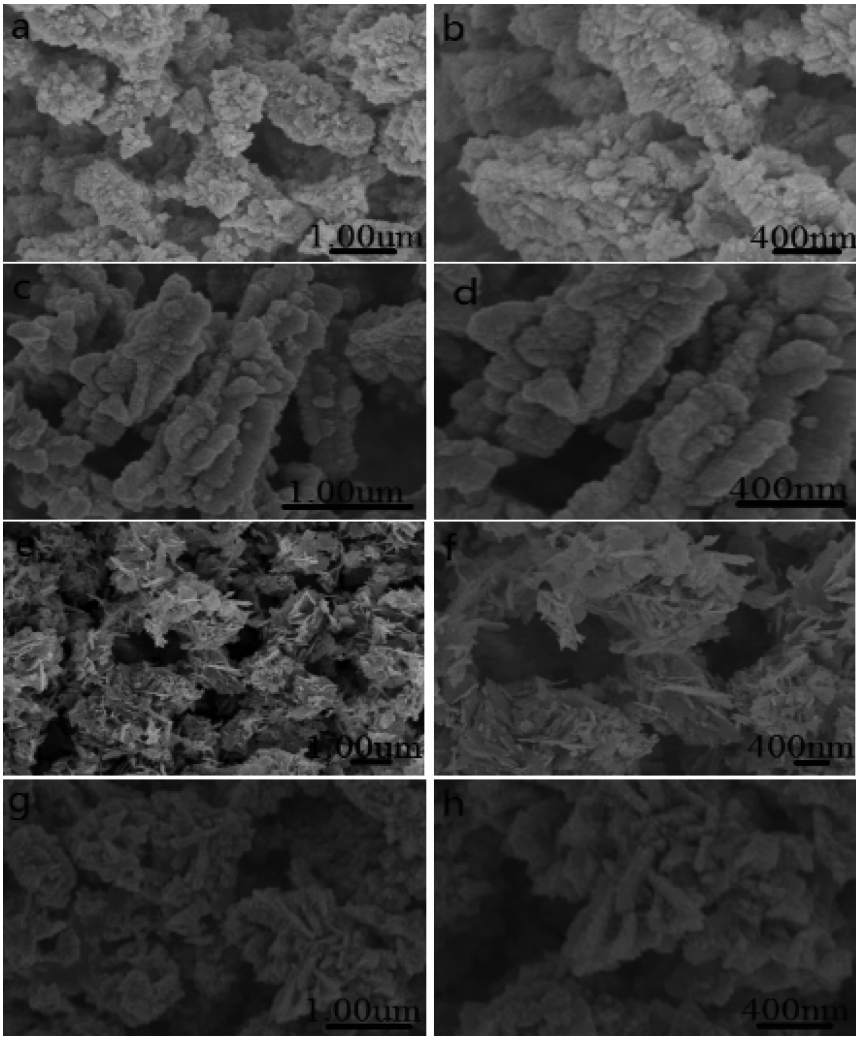


Fig.5　SEM images of ZnO samples prepared with different zinc sources

zinc source. When the mixture of zinc acetate and zinc sulfate is used as the zinc source, sample-6 formed by quasi-spherical nanoparticles presents inhomogenous size and irregular morphology (Fig.5a). It can be seen from the high-resolution image (Fig.5b) that the hierarchical structure of sample-6 is constituted by nanoparticles, and the cusp emissions are outward in the scattering form. Nevertheless, the obtained hierarchical structure of sample-7 is the agglomerate by multiple chains (Fig.5c and 5d), whose surface is unsmooth due to the nanoparticles assembly. In addition, the flake-like morphology of sample-8 can be found in Fig.5e and 5f, when the mixed zinc salts are zinc chloride and zinc nitrate. The high-resolution image (Fig.5f) of sample-8 shows the disorder hierarchical structure with wheatear-like or flower-vine morphology, some of which possess complicated structure arranged closely by the nanoflakes, while others have orderly structure arranged loosely by nanoflakes. The SEM images of sample-9 prepared by zinc chloride and zinc sulfate (Fig.5g and 5h) show some flower patterns attached by some short chains. The surface of flower patterns is rough and the shape of flower patterns is different. The high-resolution image (Fig.5h) shows that the hierarchical structure of sample-9 is similar to carved petal, and many nanoparticles adhere well on the surface of sample-9.

It can be concluded that the samples prepared by altering zinc source are different in morphology. Although the samples are hierarchical structure assembled by nanoparticles, their assembling processes are not the same, which is mainly decided by the anion in zinc salts. Throughout Fig.5, only sample-8 is not assembled by nanoparticles, i.e., $Cl^-$ and $NO_3^-$ can directly affect the growth of ZnO particles. In addition, it can be found by comparing Fig.5d with 5h that the two samples have well-organized hierarchical structures. It may be because that one crystal face of ZnO seed has a weaker absorption capacity to $Cl^-$ or $NO_3^-$, leading to the seed growth along this crystal face to form the regular grain, i.e., $Cl^-$ makes grain grow into the chain-like structure, while $NO_3^-$ makes grain grow into the flake-like structure, which may be related to anionic spatial structure and electronegativity. Interestingly, the morphology of sample-9 shown in Fig.5g is very similar to that of sample-1 (Fig.3), indicating that the effect of $SO_4^{2-}$ and $CH_3COO^-$ as the template is similar. Maybe it is because that the two anions all have larger volume and possess the three-dimensional structure, so that ZnO seed has weaker absorption on them. In addition, their larger volume may be propitious to assist the construction of the well-organized hierarchical structure.

2.3.3 Influence of temperature on the sample morphology

To study the effect of temperature on the morphology of final sample, experiments are respectively carried out at 120 and 180 ℃ under invariability of other conditions.

When the reaction temperature of the precursor solution is 120 ℃, the morphologies of the obtained sample-10 are shown in Fig.6a and 6b. It can be observed from Fig.6a that the sample-10 is thin flake-like agglomerates with irregular shape and rough surface. As shown in the high-resolution (Fig.6b), these agglomerates have the disordered structure constituted by nanoflakes with irregular shape. Some of nanoflakes are wide and short, on the contrary, others are narrow and long. On the whole, these nanoflakes are similar to the fallen leaves stacking in a mess. The nanoflake-like morphology disappears generally when the reaction temperature increases to 180 ℃, while the as-prepared sample-11 appears to be the mixed structure composing the irregular nanorods and nanoparticles aggregates (Fig.6c and 6d), and the nanoparticles of 60~100 nm attach to the nanorod surface or fill in the interspace among the nanorods. It can also be found from Fig.6d that the nanorods stack irregularly and their surface is unsmooth.

From the above results, it can be learned that the structure unit of sample-10 presents the flake-like morphology at 120 ℃. While sample-11 has two structure units including the nanorods and nanoparticles at 180 ℃. Compared with sample-1 (prepared at 150 ℃), the samples prepared at 120 and 180 ℃ have

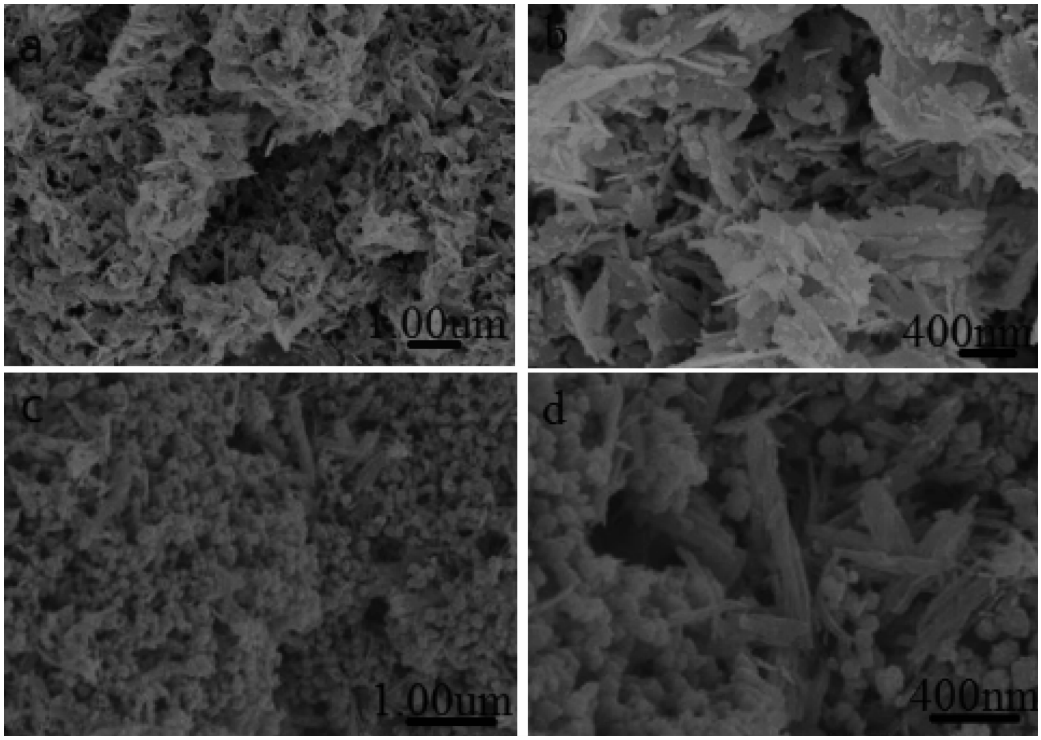


Fig.6　SEM images of ZnO samples prepared under different reaction temperature

no obvious hierarchical structure. So, the temperature plays an important role in the formation process of hierarchical ZnO. The possible reasons of this morphological difference are as follows. Firstly, the temperature has a great influence on the grain nucleation and growth rate. The nucleation rate of grain is faster than its growth rate if the temperature is too low, so the obtained grain is usually irregular under this case. On the contrast, the growth rate of grain is faster than its nucleation rate if the temperature is high enough, which is also disadvantageous to form the regular grains. When the growth rate of grain is faster than the diffusion rate of ions, the nonuniform distribution of concentration has an enormous effect on the regularity of grains. Secondly, hierarchical structure is usually assembled by small structure unit, while the assembly process needs the driving force. Hence, temperature can provide the driving force for grain assembly. But a too high temperature can dramatically enhance the Brown movement of particles, which would hinder the self-assembly of grains. On the contrary, a too low temperature can not provide enough driving force for grains assembly, which often leads to the incomplete assembly and forms disorder structure. In addition, the nano-flake is one dimensional, while the nano-rod is three dimensional in structure. So, with the increase of space dimension, the driving force needed for self-assembly is becoming greater and greater. In conclusion, sample-10 prepared under low temperature (120 ℃) presents a flake-like morphology due to lack of driving force (Fig.6a and 6b). However, owing to the enhanced Brown effect, some parts of ZnO grains form rod-like structure (Fig.6c and 6d) at high temperature (180 ℃).

### 2.4　Optical properties

Fig.7a presents the UV-Vis spectrum of the as-prepared sample-1. Compared with characteristic absorption of common ZnO (373 nm), the main absorption peak at 368 nm in Fig.7a shows some blue shift. It may be due to the nano-effect of nanoparticles on the surface of hierarchical ZnO, or the interaction between $Zn^{2+}$ and $CH_3COO^-$ absorbed by the ZnO grains making the 3*d* valence electrons of $Zn^{2+}$ transfer easily to the $\pi^*$ orbital of $CH_3COO^-$. Fig.7b shows the PL spectrum of sample-1 with the excitation wavelength

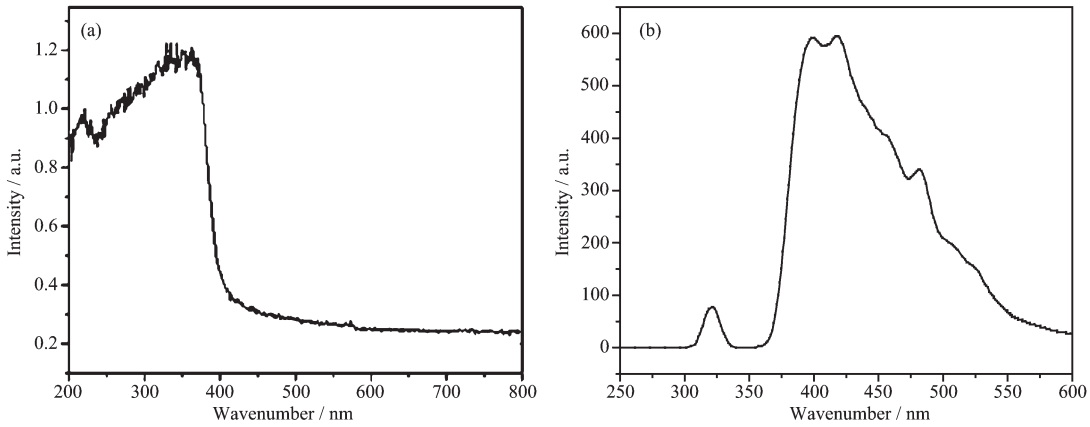


Fig.7 (a) UV-Vis diffuse reflectance spectrum and (b) PL spectrum of the sample-1

of 325 nm at room temperature. The PL spectrum possesses two emission bands, i.e. one is the narrow UV emission at about 320 nm corresponding to the electronic radiative transition from conduction band to valence band, and the other is a strong and broad emission band located in the near UV region. Furthermore, the strong double bands in 375~450 nm are the blue emission of ZnO in the visible region, one of which corresponds to the red shift and the other is the blue shift relative to central transition frequency, it may be due to the emission of excitonic recombination or the ZnO crystal defect caused by the excess $OH^-$ in the process of adding NaOH dropwise. The weak green emission at 490 nm may be caused by the electronic transition from the low energy level to valence band. Compared with the conventional ZnO nanocrystals, all emission peaks exhibit the phenomenon of blue shift to some extent. It may be because that the particles constructing the hierarchical structure belong to nano size, leading to that the emission peak position moves to the short wavelength, which provides guarantee for the improvement of photocatalytic activity.

According to literature[34], the photoluminescence property of ZnO nanoparticle associates with the oxgen vacancies and defects on ZnO surface. In the process of photoluminescence, superficial oxgen vacancies and defects can make photogenerated electron to form the free exciton or bound exciton, leading to emitting fluorescence. The more the superficial oxgen vacancies and the more defects, the highter the intensity of fluorescence will be. The representative ZnO owns the strong and broad emission band in the range of 375~550 nm as shown in Fig.7b, suggesting that hierarchical ZnO possesses more superficial oxgen vacancies and defects. However, the superficial oxgen vacancies and defects can make a large contribution to photocatalytic activity, because they can capture photogenerated electron to improve the efficiency of photoinduced charge separation.

### 2.5 Evaluation of photocatalytic activity

By experiments, the standard curve equation of MO solution is $A=0.074\ 2c+0.042\ 8$ ($R^2=0.999\ 8$, $A$/(mg·L$^{-1}$) is the solution absorbance, $c$/(mol·L$^{-1}$) is the solution concentration). The relative absorbance ($A/A_0$) of solution is considered as 1, of which MO concentration is about 12.9 mg·L$^{-1}$. In order to reach the adsorption-desorption equilibrium between the catalyst and MO, the mixed solutions including ZnO and MO have been stirred in the dark for 1 h. And $C/C_0$ values corresponding to 0 min in Fig.8 are all slightly less than 1, indicating that the three different ZnO samples have a weak absorption on MO. In the photocatalytic experiments, three kinds of as-prepared ZnO samples used as the catalyst are sample-1, sample-2, and sample-10 separately.

Fig.8 shows the photocatalytic activity of three different morphological ZnO samples on MO solution (12.9 mg·L$^{-1}$) under UV irradiation. The $C/C_0$ values of all samples decrease with increasing time (Fig.8). Obviously, the degradation rate of all samples declines gradually, and compared with sample-2 and

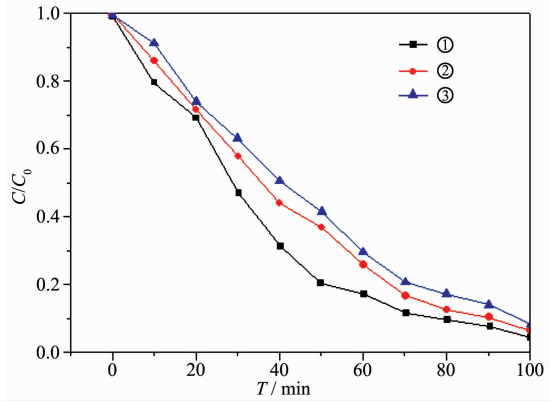


Fig.8　Photocatalytic activity of three different ZnO samples

sample-10, the degradation rate of sample-1 is the fastest. Especially, when the irradiation time is up to 100 min, only the $C/C_0$ value of sample-1 reduces to below 0.05, proving that the MO has been degraded almost completely. By contrast, the $C/C_0$ value of sample-1 is the minimum under the same irradiation time among three samples, and the photocatalytic activity of sample is the best in the whole process of photocatalytic degradation. In addition, the total organic carbon ($w$) of MO soultion degraded under sample-1 is shown in Table 2 and the relational expression is

$$w=2.310\ 3+2.0103\ 7x\ (R^2=0.999\ 66) \quad (1)$$

The w displays a dramatic variation as seen from Table 2, incidating the effective photocatalyitc activity of sample-1. Besides, the decrement of carbon ($\eta$ = 82%) is lower than the degradation rate (95%) of MO, which suggests that there are many intermediate products in the photocatalytic degradation.

**Table 2　Total content of organic carbon of MO soultion**

| | Before degradation | After degradation |
|---|---|---|
| NPOC* (Area) | 346 | 65 |
| $w$(Area) | 171 | 31 |

*NPOC=non-purgeable organic carbon, $w$=total organic carbon

It may be the hierarchical structure of sample-1 that improves the photocatalytic activity of ZnO, due to sample-2 and sample-10 without obvious hierarchical structure. So, the photocatalytic activity is closely associated with the microstructure and morphology of the catalyst.

The influence of ZnO dosage on photocatalytic activity is shown in Fig.9a. The degradation rate of MO rises generally as the increase of ZnO dosage, but the change in degradation rate is becoming slow. It may be because that when the ZnO dosage is too high, it can lead to the light scattering effect, reducing the light absorption rate of solution[35]. In addition, the inhomogenous dispersity of ZnO has also some influence on the photocatalytic activity.

To evaluate the reusability of sample-1, recycled experiments about the photocatalytic dagradation of MO have been performed. The photocatalytic activity of sample-1 is decreased to some extent after each recycle, while it still keeps above 90% after five recycles as shown in Fig.9b, suggesting that sample-1 presents excellent photocatalytic stability.

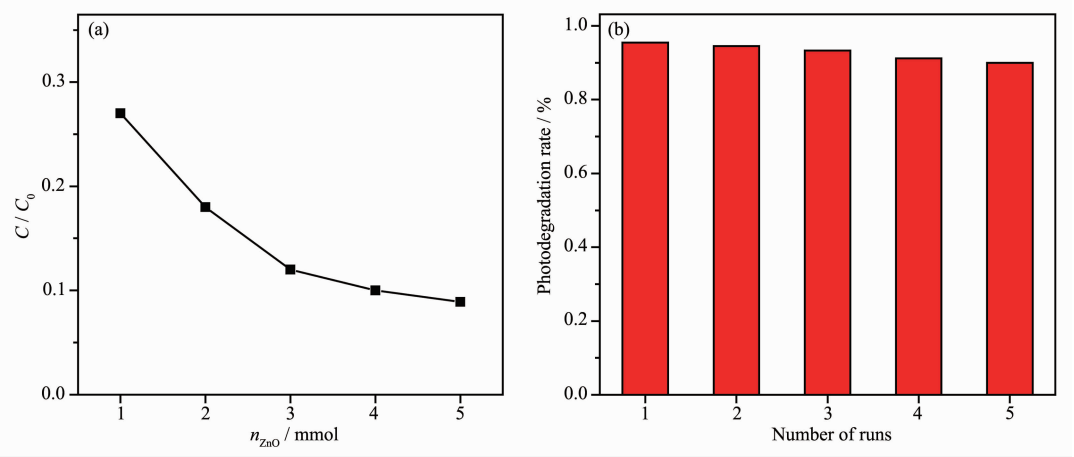


Fig.9　(a) Photocatalytic activity under different the sample-1 dosages and (b) Reusability of the sample-1 evaluated for five cycles

## 3 Conclusions

The hierarchical ZnO assembled by nanoparticles was prepared via a secondary deposition method by using the precursor solution including two zinc salts, IL and alanine as the raw materials, and the sodium hydroxide as precipitant. The as-prepared ZnO samples are hexagonal as evidenced by XRD characterization. The kind of anion and temperature plays a vital role in constructing the morphology of hierarchical structure. The combination of anion has a great influence on the sample morphology, in which $Cl^-$ and $NO_3^-$ have the directing effect on the seed growth, but the $SO_4^-$ and $CH_3COO^-$ can play the role of the template in auxiliary constructing the hierarchical structure. In addition, IL and sodium citrate working as surfactant provide an assisted function for oriented growth of ZnO grain. Moreover, sample-1 presents a strong and broad absorption, and possesses a good emission performance in the UV and near UV region as seen from the UV-Vis and PL spectrum. The photocatalytic results indicate that the photocatalytic activity of three different morphological ZnO samples is different, among which sample-1 is the best. The photocatalytic activity of ZnO is closely related to the microstructure and morphology of ZnO.

## References:


[1] WANG Xin(汪信), LU Lu-De(陆路德). *Chinese J. Inorg. Chem.*(无机化学学报), **2000**,**16**(2):213-217

[2] Ren Y, Ma Z, Bruce P G. *Chem. Soc. Rev.*, **2012**,**41**(14): 4909-4927

[3] Lee K R, Lee J H, Yoo H I. *J. Eur. Ceram. Soc.*, **2014**,**34** (10):2363-2370

[4] ZHENG Zhen-Miao(郑贞苗), TANG Xin-Cun(唐新村), WANG Yang(汪洋), et al. *Chinese J. Inorg. Chem.*(无机化学学报), **2015**,**31**(4):731-738

[5] Yuan C Z, Wu H B, Xie Y, et al. *Angew. Chem. Int. Ed.*, **2014**,**53**(6):1488-1504

[6] XU De-Kang(徐德康), LIU Chu-Feng(刘楚枫), YAN Jia-Wei(阎佳薇), et al. *Chinese J. Inorg. Chem.*(无机化学学报), **2015**,**31**(4):689-695

[7] WANG Xin-Juan(王新娟), XIAO Yang(肖洋), XU Fei(徐斐), et al. *Chinese J. Inorg. Chem.*(无机化学学报), **2014**,**30**(8): 1821-1826

[8] Sharma R K, Ghose R. *Ceram. Int.*, **2015**,**41**(1):967-975

[9] Nevosad A, Hofstatter M, Supancic P, et al. *J. Eur. Ceram. Soc.*, **2014**,**34**(8):1963-1970

[10]Qiu Z W, Yang X P, Han J, et al. *J. Am. Ceram. Soc.*, **2014**,**97** (7):2177-2184

[11]Ma S S, Li P, Lu C P, et al. *J. Hazard. Mater.*, **2011**,**192**(2): 730-740

[12]Cho S, Kim S, Jung D W, et al. *Nanoscale*, **2011**,**3**(9):3841-3848

[13]Deng S Z, Fan H M, Wang M, et al. *ACS Nano*, **2010**,**4**(1): 495-505

[14]Li H F, Huang Y H, Zhang Y, et al. *Cryst. Growth Des.*, **2009**,**9**(4):1863-1868

[15]Shang T M, Sun J H, Zhou Q F, et al. *Cryst. Res. Technol.*, **2007**,**42**(10):1002-1006

[16]Sangkhaprom N, Supaphol P, Pavarajarm V. *Ceram. Int.*, **2010**,**36**(1):357-363

[17]Gao X F, Jiang L. *Nature*, **2004**,**432**(7013):36-36

[18]Lao J Y, Wen J G, Ren Z F. *Nano Lett.*, **2002**,**2**(11):1287-1291

[19]Yang Y H, Wang B, Yang G W. *Cryst. Growth Des.*, **2007**,**7** (7):1242-1245

[20]Liu H, Li M, Wei Y, et al. *Mater. Lett.*, **2014**,**137**:300-303

[21]Huang Q, Cun T, Zuo W, et al. *Appl. Surf. Sci.*, **2015**,**332**: 581-590

[22]Shi R, Song X, Li J, et al. *Mater. Chem. Phys.*, **2015**,**156**:61-68

[23]Chang G J, Lin S Y, Wu J J. *Nanoscale*, **2014**,**6**(3):1329-1334

[24]Kokotov M, Bar-Nachum S, Edri E, et al. *J. Am. Chem. Soc.*, **2009**,**132**(1):309-314

[25]Mclaren A, Valdes-Solis T, Li G, et al. *J. Am. Chem. Soc.*, **2009**,**131**(35):12540-12541

[26]Xu S, Wang Z L. *Nano Res.*, **2011**,**4**(11):1013-1098

[27]Zhou X, Xie Z X, Jiang Z Y, et al. *Chem. Commun.*, **2005**, **44**:5572-5574

[28]Wang L, Chang L X, Wei L Q, et al. *J. Mater. Chem.*, **2011**, **21**(39):15732-15740

[29]SHEN Jun-Hai(沈俊海), LI Jia-Jia(李佳佳), LI Liang-Chao(李良超), et al. *Chem. J. Chinese Universites*(高等学校化学学报), **2014**,**35**(6):1135-1141

[30]Huddleston J G, Willauer H D. *Chem. Commun.*, **1998**,**16**: 1765-1766

[31]Brindaban C R, Subhash B. *Org. Lett.*, **2005**,**7**(14):3049-3052

[32]Fernandes D M, Silva R, Hechenleitner A A, et al. *Mater. Chem. Phys.*, **2009**,**115**(1):110-115

[33]Xing R M, Zhu J H, Liu Q W, et al. *Chem. Res.*, **2012**,**23** (5):57-60

[34]JING Li-Qiang(井立强), YUAN Fu-Long(袁福龙), HOU Hai-Ou(侯海鸥), et al. *Sci. China Ser. B*: *Chem.*(中国科学 B 辑:化学), **2004**,**34**(4):310-314

[35]HOU Chun-Yan(侯春燕). *Thesis for the Master of Dalian Maritime University*(大连海事大学硕士论文). **2006**.